

Chaotic filtering of moving atoms in pulsed optical lattices

T. Jonckheere, M. R. Isherwood and T. S. Monteiro

Department of Physics and Astronomy, University College London, Gower Street, London WC1E 6BT, U.K.

(Dated: November 20, 2018)

We propose a mechanism for a velocity-selective device, which exploits the fundamental phenomenon of dynamical localization. It would allow packets of cold atoms travelling through a pulsed optical lattice in one direction to pass undisturbed, while dispersing atoms travelling in the opposite direction. This mechanism is based on a chaotic diffusion process, with a momentum-dependent diffusion coefficient. We analyse this classical effect, and we show that it is *enhanced* by dynamical localization.

PACS numbers: 32.80.Pj, 05.45.Mt, 05.60.-k

There is much current interest in the development of new techniques to manipulate cold atoms. Recent work in atom optics has resulted in new devices termed “atom chips” [1, 2] where cold atoms may be trapped and guided by fields above a solid substrate. One might even in future envisage a multi-component chip combining arrays of micro-traps and atom wires, forming a sort of atom optics version of an integrated circuit. Within such an atom chip, techniques to, for example, split, transport and otherwise control the traffic of atoms, might play an important role.

Optical lattices in particular are receiving much current attention in atom optics, in a wide range of experimental studies. For instance, cold atoms in optical lattices have become a paradigm in the study of quantum chaos; experiments on sodium and cesium atoms [3] provided a textbook demonstration of Dynamical Localization (DL) [4, 5], the quantum suppression of classical chaotic diffusion. In these experiments the atoms experience a periodically pulsed or driven standing wave of light.

The corresponding classical motion is fully chaotic for sufficiently strong driving. This implies that the energy of the system grows diffusively with each consecutive kick: in the absence of phase-space barriers, which are present only in the regular regime, the average energy $\langle p^2 \rangle$ of the particles is unbounded and this diffusive increase in energy continues indefinitely. It is characterised by a diffusion rate D_0 , ie $\langle p^2 \rangle = D_0 t$. However in the *quantum* case this process is suppressed on the time-scale of the so-called “break-time” $t^* \sim D_0/\hbar^2$. After t^* the atoms absorb no more energy.

The series of ground-breaking experiments in [3] was followed by other experiments with optical lattices probing a wide range of quantum chaos phenomena including dynamical tunnelling [6, 7], the effect of quantum loss of coherence on dynamical localization [8] and quantum accelerator modes [9]. The experiments in [7] employed BECs in optical lattices. The dynamics of Bose-Einstein Condensates in optical lattices has recently become of very broad interest [10].

Here we show that a straightforward modification of the quantum chaos experiments can form the basis for a device to control the traffic of cold atoms moving along a

channel in, say, an atom chip by selecting a specified velocity. It was recently proposed [11] that atoms in double-well lattices, pulsed with unequal periods, will have diffusion rates which are momentum dependent: $D(p) = D_0 + C(p)$ where $C(p)$ is a momentum dependent correction. This can form the basis for a type of ratchet dynamics: for a system with zero initial momentum, $\langle p(t=0) \rangle = 0$, particles with $p > 0$, say, absorbed energy at a different rate from particles with $p < 0$, leading to a non-zero net current. While for that system $D(p)$ is locally asymmetric around $p = 0$, it has no particular symmetry over a larger scale and has complex oscillations with respect to p , with contributions from several terms. Hence it is not suitable for the velocity selector we propose here. Below we show that there is a system which has a diffusion coefficient of very simple form, with a single odd-parity correction term, ie $C(p) = -C(-p)$. For experimentally accessible parameters we can then select a regime where, for particles moving in one direction $D^+(p) = D_0 + C(p) \sim 0$ which means they absorb little or no energy; while particles moving in the opposite direction experience an enhanced diffusion rate $D^-(-p) > D_0$. While in the classical case, this effect is confined to a narrow parameter range, we show here that for the equivalent quantum system, this “filtering effect” is in fact substantially *enhanced* by DL relative to the classical case, and remains effective over a wider parameter range. We investigated DL in this anomalous diffusion regime and find that it is associated with a local “break-time” $t^*(p) \sim D(p)/\hbar^2$. The ratio of energy absorbed by particles moving in opposite directions, classically is $\sim D^+(p)/D^-(p)$ for short times and ~ 1 for large t ; in the quantum case, due to dynamical localization, the corresponding ratio is $[D^+(p)/D^-(p)]^2 \sim cst$ for $t > t^*$. If implemented, this would represent an atom optics application of what to date remains a much studied fundamental physics phenomenon.

In the dynamical localization experiment of [3, 6, 8], the dynamics is approximately given by the kicked-particle Hamiltonian : $H = \frac{p^2}{2} - K \cos x \sum_n \delta(t - nT)$ where K is the kick strength. The classical dynamics is obtained by iterating the well-known “Standard Map”: $x_{i+1} = x_i + p_i T$; $p_{i+1} = p_i + K \sin x_{i+1}$. In the Standard Map, we can take $T = 1$, without loss of generality, but

for the proposed system, we use a repeating cycle of unequally spaced kicks. For simplicity, we take a length-2 cycle, with the spacing between kicks alternating between T_1 and T_2 . The Hamiltonian is now given by :

$$H = \frac{p^2}{2} + V(x) \sum_{n=0}^{\infty} \sum_{M=1}^2 \delta(t - nT_{tot} + \sum_{i=1}^M T_i) \quad (1)$$

with $T_{tot} = T_1 + T_2$. This means that the first kick after $t = 0$ is at $t = T_1$, the second kick at $t = T_1 + T_2$, the next one at $t = T_1 + (T_1 + T_2)$ and so on. We will consider only a small deviation from equally spaced kicks, which can be defined with the small parameter b , $T_1 = 1 + b$, $T_2 = 1 - b$. The spatial symmetry is broken by a linear term which alternates in sign: $V(x) = -(K \cos x + Ax(-1)^j)$ where j is the kick number. This Hamiltonian leads to the map:

$$\begin{aligned} x_i &= x_{i-1} + p_{i-1}(1 + b) \\ p_i &= p_{i-1} + K \sin x_i + A \\ x_{i+1} &= x_i + p_i(1 - b) \\ p_{i+1} &= p_i + K \sin x_{i+1} - A \end{aligned}$$

This classical map was investigated previously [12] in the regular regime. Here we have investigated the properties of this map in the chaotic regime. We have also investigated the equivalent quantum behaviour. Since the Hamiltonian involves only delta-kicks, we consider the usual time evolution operator in a matrix representation using a plane-wave basis. We find that while single kicks couple different quasimomenta, the combined time evolution operator for two kicks does not. Hence it is most convenient to iterate the two-kick time-evolution operator. In the usual plane-wave basis $|n\rangle = \frac{1}{2\pi} \exp(inx)$ this takes the form of a matrix $\hat{U}(2)$ with elements:

$$\begin{aligned} \langle n | U^q | l \rangle &= e^{-i((1+b)(l+q)^2\hbar)} \\ &\sum_j e^{-i(1-b)(j+qa)^2\hbar} J_{l-j+ka}(\frac{K}{\hbar}) J_{j-n-ka}(\frac{K}{\hbar}) \quad (2) \end{aligned}$$

where q is a quasimomentum, $ka = \text{int}(q - A)$ and $qa = q - A - ka$. We solve for the quantum time evolution by simply iterating repeatedly $\psi(2) = \hat{U}\psi(t=0)$. In Fig. 1 we demonstrate the effect on two quantum wavepackets by iterating Eq. (2) over 50 pairs of kicks for two different sets of parameters ($K = 2.0$ and $\hbar = 0.25$ for (a), $K = 3.2$ and $\hbar = 1.0$ for (b)). We show that the device functions as a sort of Maxwell demon: while packets moving to the right pass the pulsed lattice relatively unperturbed, those moving to the left are strongly dispersed. Below we analyse this effect.

For the Standard Map, at the lowest level of approximation, the classical momenta at consecutive kicks are uncorrelated and evolve in time as a ‘‘random-walk’’. This means that the average momentum of a large ensemble of particles is unchanged, and that the average

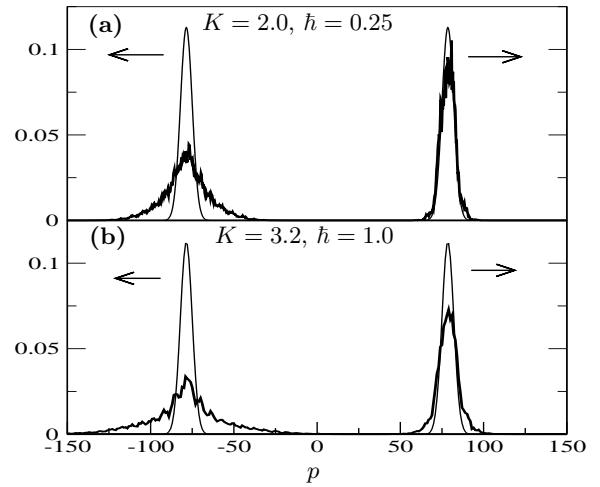


FIG. 1: Demonstration of the filtering effect: figure compares the effect of 50 pairs of pulses on two quantum wavepackets moving in opposite directions. Initial wavepackets are shown with a thin line, while the final wavepackets are shown with a bold line. Parameters : (a) for kick strength $K = 2.0$, $\hbar = 0.25$, (b) for $K = 3.2$, $\hbar = 1.0$. The values of A and b are, in both cases, $\pi/2$ and 0.01 respectively. The initial wavepackets are centred around $\pm p_0$, with $4bp_0 = \pi$. The initial widths of the wavepackets are similar to the experimental values. The figure shows that while the right-moving wavepacket is only slightly perturbed, the left-moving one is strongly dispersed.

energy grows linearly: the average kinetic energy $\langle p^2 \rangle / 2$ grows by $K^2/4$ at each consecutive kick. In the absence of phase-space barriers the energy is unbounded and this diffusive increase in energy continues indefinitely. It is characterised by a diffusion rate D_0 , ie $\langle p^2 \rangle = D_0 t$ so for uncorrelated momenta $D_0 = K^2/2$. However, correlations between sequences of consecutive kicks give important corrections to the diffusion coefficient. The 2-kick correlation for example, originates from correlations between adjacent kicks but one, $\langle V'(x_i)V'(x_{i-2}) \rangle$, and gives a correction $-K^2 J_2(K)$ to the diffusion coefficient. The diffusion coefficient, including the first corrections, is: $D_0 = K^2(1/2 - J_2(K) - (J_1(K))^2 + \dots)$ [13, 14]. These corrections have even been measured experimentally with cold cesium atoms in pulsed optical lattices [15].

For the Hamiltonian in Eq. (1), the correlations take a modified form. The corrections they induce are now momentum dependent: for an ensemble of particle with initial momentum p_0 , the average energy spread at time t is given by

$$\begin{aligned} \langle (p - p_0)^2 \rangle &= K^2 t \left(\frac{1}{2} - \frac{1}{2} [J_1(K(1+b))^2 + J_1(K(1-b))^2] \right) \\ &\quad - K^2 \Phi(t) C(2, p_0) + \dots \quad (3) \end{aligned}$$

Where

$$\begin{aligned} C(2, p_0) &= J_0(2bK) \cos(2p_0 b - A(1-b)) \\ &\quad [J_2(K(1+b)) + J_2(K(1-b))] \end{aligned}$$

and

$$\Phi(t) = \frac{1 - J_0(2bK)^{t-2}}{1 - J_0(2bK)^2}$$

Higher order correlations (4-kick, etc.) involve more Bessel functions, and induce corrections that may become significant over part of the parameter range, but eq. (3) has the main features. The first correction in equation (3) is due to 3-kick correlation, and is very similar to the $J_1(K)^2$ correction for the standard map. The $C(2, p)$ term is the modified version of the 2-kick correlation term which for the standard map took the form $-K^2 J_2(K)$. This term has several important properties. Firstly, it is p -dependent with the $\cos(2pb - (1 - b)A)$ term. This means that particles with different momenta will absorb energy at different rates. This feature is the basis of the filtering effect shown above. Secondly, it has a non trivial time-dependence, given by the function $\Phi(t)$. Since $bK \ll 1$, one has $J_0(2bK) \simeq 1 - (bK)^2$. For $t \ll 1/(bK)^2$, $\Phi(t)$ has a linear behaviour ($\sim t/2$), and the $C(2, p)$ term appears as a correction to the diffusion coefficient, as in the standard map. However, for larger t , $\Phi(t)$ saturates to the value $(bK)^2/2$, and the 2-kick correlation does not modify the energy growth anymore.

All the expressions simplify considerably if we consider that $b \sim 0.01$ is a small deviation from period-one pulses, so $bA, bK \ll 1$. For times $t \ll 1/(bK)^2$, we can write:

$$\langle (p - p_0)^2 \rangle = K^2 t \left[\frac{1}{2} - J_1(K)^2 - J_2(K) \cos(2p_0 b - A) \right] \quad (4)$$

Hence we have a local diffusion coefficient of the form $D(p) \simeq D_0 - C(2, p)$, where $D_0 \simeq K^2[1/2 - J_1(K)^2]$.

Figure 2 shows a comparison of this formula to numerical results: the average energy spread after 20 kicks is plotted as a function of K , for an ensemble of 400,000 particles with a narrow initial momentum distribution around $p_0 = \pi/(4b)$, with $b = 0.005$ and $A = \pi/2$. For these values, one has $\cos(2p_0 b - A) = 1$. For clarity, we have removed the p -independent contribution D_0 . We see that the numerical results agree very well with the formula (4), showing the $J_2(K)$ oscillations. For the larger values of K shown on the figure, the effect of the function $\Phi(t)$ begins to be noticeable, and formula (4) overestimates the result. The full analytic formula (3) is also shown, with an excellent agreement over the whole range of K .

Figure 3, (a) and (b), shows the average energy spread as a function of the initial momentum p_0 , for two different sets of parameters. In each case both the classical and the quantum results are shown. For the classical case (dotted line on the figure) we obtain, as expected from eq. (4), a cosine behaviour in p_0 , with a period π/b . The quantum results (full curve) are similar to the classical one. In (a), the number of kicks has been chosen to obtain the same maximum energy spreading for the quantum and

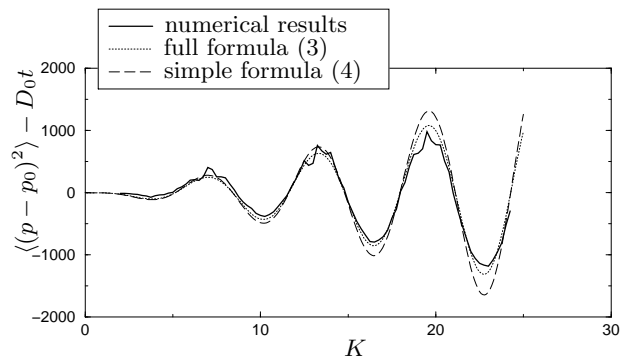


FIG. 2: Average energy spread as a function of K , for an ensemble of 400,000 particles with a narrow initial momentum distribution around $p_0 = \pi/(4b)$, with $b = 0.005$ and $A = \pi/2$. The $D_0 t$ term has been removed (see text). The numerical results are compared to the simple formula (4), valid for $t \ll 1/(bK)^2$, and to the full analytical formula (3).

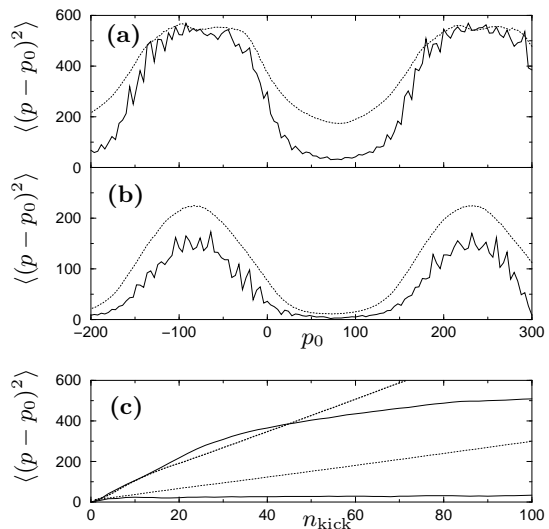


FIG. 3: (a)-(b): average energy spread as a function of initial momentum, in the classical case (dotted curve) and the quantum case (full curve). The parameters are: (a) $K = 3.2$, $\hbar = 1$, 60 kicks for the classical curve, 200 kicks for the quantum curve; (b) $K = 1.7$, $\hbar = 0.25$, 100 kicks for the classical curve, 100 kicks for the quantum curve. In both case, $A = \pi/2$ and $b = 0.01$. In (a), the number of kicks in the classical case has been chosen to obtain the same maximum value for the energy spread as in the quantum case. The results show clearly that the diffusion coefficient oscillates as a function of p , with period π/b , and that the minimum of the diffusion coefficient is lowered in the quantum case compared to the classical one.

(c) Average energy spread as a function of kick number, for two wavepackets: one initially centred around $p_0 = \pi/(4b)$ (the two lower curves), the other initially centred around $p_0 = -\pi/(4b)$ (the two upper curves). The classical results are shown as dotted curves, while the quantum results are shown as full curves. One can see that the quantum wavepacket with slow energy spread localizes extremely quickly, while the other wavepacket takes a much longer time to localize. Parameters: $K = 3.2$, $b = 0.01$, $A = \pi/2$ and $\hbar = 1$ in the quantum case.

the classical results; this shows clearly that the quantum minimum of the energy spreading is much lower than the classical one.

This quantum effect is due to dynamical localization: near a maximum or a minimum of the $\cos(2p_0b - A)$ function, the classical diffusion coefficient is enhanced or reduced, respectively. Since the break-time, which gives the time needed by the quantum system to localize, is proportional to the diffusion coefficient, one sees that near a maximum of the diffusion coefficient, the quantum system takes longer to localize, and thus the quantum wavepacket absorbs energy for a longer time. On the other hand, near a minimum of the diffusion coefficient, the quantum system localizes more quickly, and the quantum wavepacket absorbs energy for a shorter time. More quantitatively, this means that the break time now depends on initial momentum: $t^*(p_0) \sim D(p_0)/\hbar^2$. As a consequence, if the ratio of the maximum and minimum classical diffusion coefficient (or energy spread) is of the order of D_+/D_- , then for the quantum system we expect a ratio for the energy spread of the order of $(D_+/D_-)^2$. In fig. 3 (a) ($K = 3.4$) for example, the ratio D_+/D_- is roughly of the order of 3, while the ratio of the quantum energy spreads is roughly 9. This enhancement due to dynamical localization is further illustrated on fig. 3 (c), where the energy of the two wavepackets

(one initially centred around $p_0 = \pi/(4b)$ (minimum), the other around $p_0 = -\pi/(4b)$ (maximum)) is plotted as function of the kick number, for the classical and the quantum case, for $K = 3.4$. One sees that the quantum wavepacket with the slowest energy spread localizes very quickly (a few kicks are enough), while the other wavepacket takes a much longer time to localize.

In sum, the filtering device results from a combination of two physical processes. Firstly, a momentum-dependent diffusion coefficient of a particular simple form which enables one to select the velocities of interest by adjusting the sign and magnitude of b (in the range $b \sim 0.05 - 0.01$ typically). Secondly dynamical localization, which enhances the classical effect by localizing quickly (slowly) the quantum wavepacket which absorbs energy slowly (fast). While this quantum filter works well over the range $K \sim 1.5 - 3.5$ the corresponding classical one is effective only for a restricted number of kicks and over a narrower range of $K \sim 1.5 - 1.8$. The parameter ranges of K and \hbar ($\hbar \sim 0.25 - 1.0$) are accessible with current experiments.

T.M. thanks Thomas Dittrich, Sergej Flach and Holger Schanz for helpful discussions. M.I acknowledges an EPSRC studentship. The work was supported by EPSRC grant GR/N19519.

-
- [1] E.A. Hinds, C.J. Vale and M.G. Boshier, Phys. Rev. Lett. **86**, 1462 (2001)
 - [2] W. Hänsel, P. Hommelhoff, T. W. Hänsch and J. Reichel, Nature **413**, 498 (2001)
 - [3] F.L. Moore, J.C. Robinson, C.F. Bharucha, Bala Sundaram and M.G. Raizen, Phys. Rev. Lett. **75**, 4598 (1995)
 - [4] G. Casati, B.V. Chirikov, Izraelev F.M. and J. Ford in "Lecture notes in Physics", Springer, Berlin **93**, 334 (1979)
 - [5] S. Fishman, D.R. Grempel and R.E. Prange, Phys. Rev. Lett. **49**, 509 (1982)
 - [6] D.A. Steck *et al.*, Science **293**, 274 (2001)
 - [7] W.K. Hensinger *et al.*, Nature **412**, 52 (2001)
 - [8] B.G. Klappauf, W.H. Oskay, D.A. Steck and M.G. Raizen, Phys. Rev. Lett. **81**, 1203 (1998)
 - [9] M.B. d'Arcy, R.M. Godun, M. Oberthaler, D. Cassetari and G.S. Summy, Phys. Rev. Lett. **87**, 074102 (2001)
 - [10] M. Greiner, O. Mandel, T. Esslinger, T.W. Hänsch and I. Bloch, Nature **415**, 39 (2002)
 - [11] T.S. Monteiro, P.A. Dando, N.A.C. Hutchins and M.R. Isherwood, Phys. Rev. Lett. **89**, 194102 (2002)
 - [12] T. Cheon, P. Exner and P. Seba, preprint, cond-mat/0203241, 12 March 2002
 - [13] A.J. Lichtenberg and M.A. Lieberman, *Regular and Chaotic Dynamics*, Springer-Verlag, New York (1992)
 - [14] D. L. Shepelyansky Phys. Rev. Lett. **56**, 677 (1986)
 - [15] B.G. Klappauf, W.H. Oskay, D.A. Steck and M.G. Raizen, Phys. Rev. Lett. **81**, 4044 (1998)